Local and nonlocal curvature elasticity in bilayer membranes by tether formation from lecithin vesicles

Richard E. Waugh,* Jianben Song,* Saša Svetina,‡ and Boštjan Žekš‡
*Department of Biophysics, University of Rochester School of Medicine and Dentistry, Rochester, New York 14642 USA; and
‡Institute of Biophysics, Medical Faculty and "J. Stefan" Institute, University of Ljubljana, 61105 Ljubljana, Lipičeva 2, Slovenia

ABSTRACT Bilayer membranes exhibit an elastic resistance to changes in curvature. This resistance depends both on the intrinsic stiffness of the constituent monolayers and on the curvature-induced expansion or compression of the monolayers relative to each other. The monolayers are constrained by hydrophobic forces to remain in contact, but they are capable of independent lateral redistribution to minimize the relative expansion or compression of each leaflet. Therefore, the magnitude of the expansion and compression of the monolayers relative to each other depends on the integral of the curvature over the entire membrane capsule. The coefficient characterizing the membrane stiffness resulting from relative expansion is the nonlocal bending modulus k_r. Both the intrinsic (local) bending modulus (k_c) and the nonlocal bending modulus (k_r) can be measured by the formation of thin cylindrical membrane strands (tethers) from giant phospholipid vesicles. Previously, we reported measurements of k_c based on measurements of tether radius as a function of force (Song and Waugh, 1991, *J. Biomech. Engr.* 112:233). Further analysis has revealed that the contribution from the nonlocal bending stiffness can be detected by measuring the change in the aspiration pressure required to establish equilibrium with increasing tether length. Using this approach, we obtain a mean value for the nonlocal bending modulus k_r of $\sim 4.1 \times 10^{-19}$ J. The range of values is broad ($1.1–10.1 \times 10^{-19}$ J) and could reflect contributions other than simple mechanical equilibrium. Inclusion of the nonlocal bending stiffness in the calculation of k_c results in a value for that modulus of $\sim 1.20 \pm 0.17 \times 10^{-19}$ J, in close agreement with values obtained by other methods.

INTRODUCTION

A number of biological processes require the formation and deformation of bilayer membranes at high curvature. Fusion of intracellular transport vesicles during endocytosis and membrane biosynthesis (25), the formation of tubulovesicular processes of the Golgi and the endoplasmic reticulum (3, 4, 14), and release of neurotransmitters at the neural synapse (20) are a few notable examples. An understanding of the physical characteristics of the membrane and its resistance to deformation is essential for understanding these processes at a fundamental level.

Bilayer membranes have been well described as two-dimensional fluids: they exhibit a strong resistance to changes in their surface area, but readily undergo surface shear deformations at constant surface area. In addition, the bilayer exhibits an elastic resistance to changes in curvature. Quantitative descriptions of membrane properties were developed by Evans and coworkers (7, 10), Helfrich (13), and others. Because of its lamellar structure, the resistance of the membrane to bending is complex. It is due in part to the intrinsic resistance of the individual monolayers to changes in curvature in a local region. In addition, there is a contribution due to the expansion/compression of the outer/inner monolayer when the bilayer bends. The contribution from such curvature-induced changes in monolayer area is a nonlocal effect because the monolayers are capable of independent lateral redistribution to equalize the area per molecule of each leaflet over the entire surface of the membrane. Therefore, the net contribution depends on the integral of the membrane curvature over the entire membrane capsule (2, 6). The qualitative aspects of this behavior were first popularized by Sheetz and Singer (18). Quantitative descriptions of this characteristic, that bending resistance depends on both the local curvature as well as the integral of the curvature over the whole surface, were developed by Evans (6) and by Helfrich (12), and subsequently analyzed by Svetina et al. (21, 22). The nonlocal resistance to bending is described as the "relative expansivity" of the constituent monolayers. An intrinsic modulus, the nonlocal bending modulus (k_r), characterizes the membrane stiffness arising from the bending-induced changes in monolayer area (12).

Measurement of the membrane bending stiffness is difficult because it is very small. A number of groups have used observations of thermally-driven fluctuations of the membrane contour to deduce a value for the bending coefficient (5, 11, 16, 17). However, interpretation of these observations is not straightforward. A

Address correspondence to Richard E. Waugh, Department of Biophysics, University of Rochester Medical Center, 601 Elmwood Avenue, Rochester, NY 14642.

0006-3495/92/04/974/09 $2.00

number of factors other than the local bending stiffness (e.g., relative expansion of the constituent monolayers and the constraints of constant vesicle surface area and volume) influence the nature of the fluctuations. In addition, the calculated coefficient depends on the assumptions of the model used to interpret the data. Consequently, the values obtained from such measurements vary over a wide range ($0.4–3.0 \times 10^{-19}$ J). More recently, Evans and Rawicz (9) have developed an approach using micropipettes to measure the membrane tension generated by thermal fluctuations. The method takes advantage of the fact that the magnitude of the fluctuations and the corresponding lateral tension depend on the availability of excess membrane area. This method properly accounts for the constraints on area and volume and avoids the experimental difficulties of trying to resolve small movements of the nearly invisible membrane. They obtain a value for k_c of $\sim 0.9 \times 10^{-19}$ J for stearoyl-oleoylphosphatidylcholine (SOPC) membranes.

Another approach for measuring the membrane bending stiffness involves the formation of thin cylinders of membrane (tethers) from large thin walled phospholipid vesicles (1, 19). This approach was developed after theoretical analysis of the equilibrium of a membrane cylinder under an axial load led to the prediction that the radius of the cylinder (tether) R_t should be inversely proportional to the axial force f, and that the coefficient relating these two quantities is the membrane bending stiffness k_c (24):

$$f = \frac{2\pi k_c}{R_t}. \tag{1}$$

An estimate of the nonlocal bending contribution to these measurements indicated that under typical conditions, it would be small. Consequently, the relative expansion and compression of the constituent monolayers was neglected in the interpretation of those measurements. Recent measurements of k_c for phosphatidylcholine-phosphatidylserine (PC-PS) mixtures gave a value of $\sim 1.6 \times 10^{-19}$ J, that was independent of the concentration of charged lipid (PS) in the membrane (19).

In a companion report, the importance of curvature-induced changes in monolayer area during tether formation is analyzed in detail. Inclusion of the nonlocal bending rigidity affects the calculated value of the bending stiffness k_c, the condition of equilibrium between the force on the tether and the suction pressure in the micropipette, and the calculation of the tether radius. In this report, we take advantage of the predicted influence of nonlocal bending resistance on the conditions of equilibrium to estimate the nonlocal bending modulus of the membrane. We use our measurement of the nonlocal bending coefficient (γ) to improve our calculation of k_c from these measurements.

THEORETICAL BACKGROUND

The differential of the free energy functional used to derive the conditions of equilibrium for tether formation at constant membrane area is (see Eq. 12 in reference 2):

$$dF = \pi k_c\, d\left(\frac{L_t}{R_t}\right) - f\, dL_t - \pi R_p^2 \Delta p\, dL_p + \gamma(L_t - L_t^*)\, dL_t, \tag{2}$$

where L_t and R_t are the length and radius of the tether, L_p is the length of the projection in the pipette, R_p is the pipette radius, R_v is the radius of the vesicle, f is the force on the tether and Δp is the difference in pressure between the inside of the pipette and the surrounding medium. (The change in energy associated with membrane area dilation during tether formation can be neglected [see reference 2 and Appendix 2]). The first term represents the elastic energy storage due to the intrinsic (local) bending elasticity of the membrane. The second and third terms represent the work done by the external forces: the force on the tether and the aspiration pressure, respectively. The last term contains the contribution from nonlocal bending resistance. It is recognized that as the tether forms, the inner monolayer is progressively compressed and the outer monolayer is expanded. The fractional change in the areas of the two leaflets resulting from the tether formation increases approximately linearly with the tether length (2). The quantity L_t^* is introduced to account for the possibility that there may be a difference between the areas of the two leaflets before tether formation. Such a difference would result in a tendency for the membrane to form a tether (of length L_t^*) that would alleviate this difference. The coefficient γ is an extrinsic factor which, in this analysis, is assumed to depend only on the intrinsic nonlocal bending modulus k_r and the total area of the vesicle, A:

$$\gamma = \frac{4\pi^2 k_r}{A}. \tag{3}$$

The nonlocal bending modulus is expected to depend on the area expansivity modulus of the bilayer (K) and the square of the separation of the neutral surfaces of the constituent monolayers (h) (21):

$$k_r = \frac{Kh^2}{4}. \tag{4}$$

The equilibrium conditions are obtained by minimizing the free energy functional subject to the constraints of constant vesicle area and volume. Two independent equations are obtained (2):

$$f_{eff} = \frac{2\pi k_c}{R_t} + \gamma L_t \tag{5}$$

$$\Delta p = \frac{k_c}{R_t^2}\left(\frac{1}{R_p} - \frac{1}{R_v}\right), \tag{6}$$

where the effective force f_{eff} is defined as (2):

$$f_{eff} = f + \gamma L_t^*. \tag{7}$$

These equilibrium equations are identical to those obtained previously (1), but with the additional terms containing the nonlocal bending coefficient γ. The quantities k_c, γ, $f_{eff}(L_t^*)$, and R_t are to be determined

from the measured values for f, R_p, R_{vo} (the vesicle radius when $L_t = 0$), R_p, and the dependence of L_p and Δp on L_t.

METHODS

The procedures for making vesicles and forming tethers are described in detail elsewhere (19). The lipids, 1-stearoyl-2-oleoyl-phosphatidylcholine (SOPC), and 1-palmitoyl-2-oleoyl-phosphatidylserine (POPS) were obtained from Avanti Polar Lipids (Birmingham, AL). Lipids were mixed to the desired proportions, dried onto a teflon surface, then rehydrated in 100 mM sucrose and allowed to stand at room temperature for 2–5 d. On the day of the experiment, the vesicles were dispersed into 110 mM glucose containing 10 μM NaCl and placed in a vertical chamber in the stage of a microscope oriented so that the optical axis was horizontal. Between the second and fifth days after rehydration of the lipids, an adhesive contact could be obtained between the vesicle and a small (10–30 μm diameter) glass bead. The vesicle-bead pair was picked up with a micropipette (7.0–10.0 μm inside diameter [ID]) and positioned in the chamber. When the aspiration pressure in the pipette holding the vesicle was reduced below a critical value, the bead fell away from the vesicle forming a strand of membrane (tether) between the bead and the body of the vesicle. By adjusting the aspiration pressure to an appropriate value, the bead could be stopped at any desired tether length. Thus, the aspiration pressure at equilibrium could be measured as a function of the tether length. The process of tether formation was reversible, and several series of measurements for increasing and decreasing tether length were performed on each tether. The aspiration pressure was set using a micrometer drive to adjust the height of a water-filled reservoir connected to the back of the pipette by a continuous water-filled pathway. The experiments were recorded on video tape, and the micrometer setting at each equilibrium point was recorded in the video image. The recordings were played back to obtain the dimensions of the vesicle and the change in the length of the projection in the pipette as a function of the tether length. Changes in the equilibrium pressure could be resolved to less than 0.1 mm H_2O (10 dyn/cm^2). The absolute magnitude of the aspiration pressure (i.e., the pressure difference between the pipette interior and the chamber) was subject to greater uncertainties because the pressure in the chamber was affected by changes in the depth of the suspending fluid or in the curvature of the interface at the top of the chamber where the pipette was inserted. Some drift in the zero pressure was typically observed because of evaporation or "settling" of the fluid in the chamber. It was essential to perform multiple series of measurements to ensure that the changes in pressure observed at different tether lengths were not the result of changes in the zero pressure. If the changes in pressure with L_t were not reproducible, the data were discarded.

Calculations. To calculate the coefficients γ, k_c, and f_{eff} from the data, it was first necessary to obtain expressions for these coefficients in terms of the measured parameters. These relationships (derived in Appendix 1) take the following form:

$$f_{eff} = -2\pi\Delta p R_p^2 \left(\frac{dL_p}{dL_t}\right) \tag{8}$$

$$\gamma = \frac{X f_{eff}}{\Delta p + X L_t}, \tag{9}$$

and

$$k_c = \frac{(f_{eff} - \gamma L_t)^2}{4\pi^2 \Delta p}\left(\frac{1}{R_p} - \frac{1}{R_v}\right), \tag{10}$$

where in Eq. 9

$$X = \frac{f_{eff} R_p}{16\pi R_v^3 (R_v - R_p)} - \frac{1}{2}\frac{d\Delta p}{dL_t}. \tag{11}$$

It should be noted that in Eq. 11, the second term is typically an order of magnitude larger than the first term. Thus, the value of γ depends primarily on the derivative, $d\Delta p/dL_t$. Knowing the effective force f_{eff} the parameter L_t^* can be calculated via Eq. 7.

The values for pressure and projection length at $L_t = 0$, Δp_o and L_{po}, and the slopes $d\Delta p/dL_t$ and dL_p/dL_t were determined by linear regression. In fact, the slope dL_p/dL_t is not constant, but the linear regression gives an accurate measure of the slope at the midpoint of the pull. Therefore, the parameters were evaluated at the "average" tether length L_{tav}, halfway between the minimum and the maximum measured values. The values for Δp and Lp at L_{tav} were calculated from the linear regressions:

$$L_{pav} = L_{po} + \frac{dL_p}{dL_t} L_{tav} \tag{12}$$

$$\Delta p_{av} = \Delta p_o + \left(\frac{d\Delta p}{dL_t}\right) L_{tav}. \tag{13}$$

The vesicle radius at the midpoint is calculated from L_{pav} and the measured values for R_v and L_p at an initial reference state (R_{vi} and L_{pi}). The condition of constant vesicle volume requires that:

$$R_{vav}^3 = R_{vi}^3 + \frac{3}{4} R_p^2 (L_{pi} - L_{pav}). \tag{14}$$

At constant force, the tether radius is expected to increase with increasing tether length (Eq. 5). This is reflected by an increasingly negative slope in the relationship between L_p and L_t (see Figs. 5 *A* and 6 *A* in reference 2). The theoretical relationship between L_t and L_p takes the form:

$$L_p = L_{po} + \frac{4}{3}\frac{R_{vo}^3}{R_p^2}\left(1 - \left[\frac{(1 - \gamma L_t/f_{eff})^2 (1 - b\Delta p_o)}{(1 - \gamma L_t/f_{eff})^2 - b\Delta p}\right]^3\right), \tag{15}$$

where the constant coefficient b is:

$$b = \frac{4\pi^2 R_p k_c}{f_{eff}^2}. \tag{16}$$

Eq. 15 reveals that the curvature of the L_p vs. L_t relationship (i.e., terms that are second order or higher in L_t) depends primarily on the ratio of the coefficient γ to the force f_{eff}. (In reference 2, γ is contained in the parameter $q = k_t/k_c$.)

RESULTS

Measurements were obtained from 22 different tethers formed from SOPC vesicles with either 2.0% ($n = 9$) or 10.0% ($n = 13$) POPS. The dependence of the equilibrium pressure on tether length for two typical vesicles is shown in Fig. 1. Data from three successive pulls for each vesicle are shown. The theoretical prediction for the relationship between pressure and tether length shows a slight upward curvature (2), but precision of our

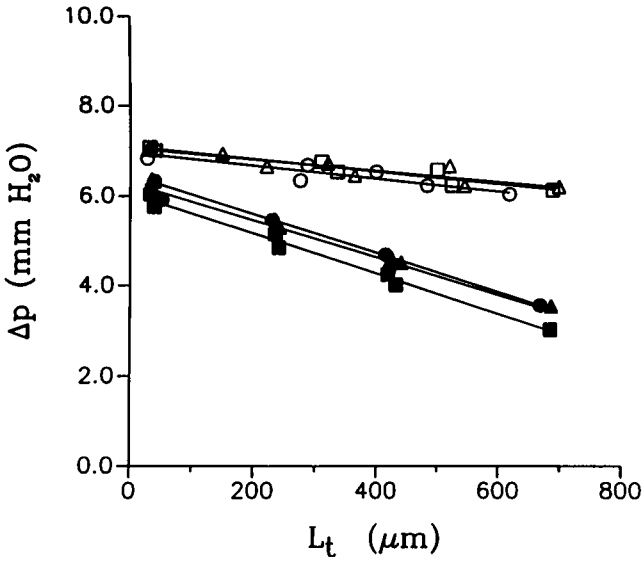

FIGURE 1 The aspiration pressure at equilibrium (Δp) as a function of the tether length (L_t). Open and filled symbols represent data from two different tethers, and different symbols designate data from three successive pulls on each tether. The solid lines represent the linear regressions to the data. The values for γ obtained from these data sets were 5.2×10^{-6} dyn/cm (*open symbols*) and 17.1×10^{-6} dyn/cm (*filled symbols*).

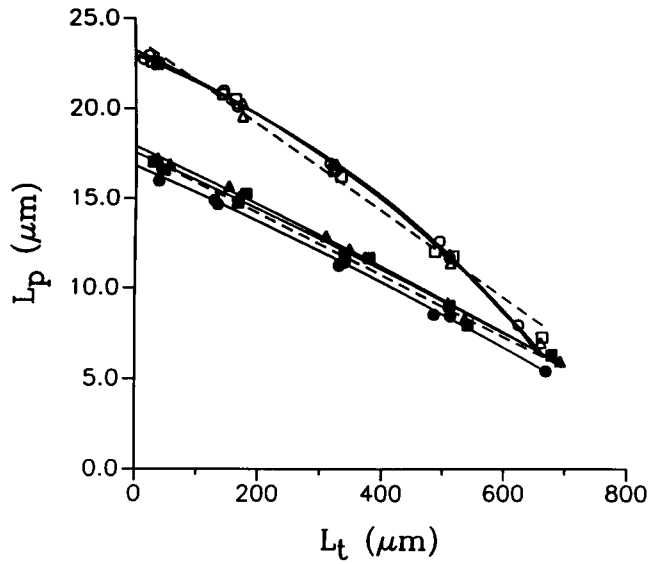

FIGURE 2 The length of the projection of the vesicle in the pipette (L_p) as a function of the tether length (L_t). Open and filled symbols represent data from three successive pulls on each of two different tethers. The solid curves show the theoretical prediction for the dependence of L_p on L_t given by Eqs. 15 and 16. Note the excellent agreement between the data and the prediction. Dashed lines show a linear regression to the data. The values for the tether radius at the midpoint of the curve ($L_t = \sim 350$ μm) obtained from these two data sets were 37.0 nm (*open symbols*) and 31.0 nm (*filled symbols*).

pressure measurements was insufficient to test this prediction. Within the resolution of the measurements, the change in pressure with tether length was linear. Note that the equilibrium pressure at a given tether length is nearly the same from one pull to the next. Data that did not exhibit this consistency were discarded. For 3 of the 22 vesicles tested, data from only 1 pull were obtained, and stability of the pressure could not be confirmed. Of the 19 vesicles for which data from 2 or more pulls were obtained, 4 were rejected because of apparent instabilities in the pressure. The reported data include only the remaining 15 vesicles.

The dependence of L_p on tether length is shown in Fig. 2. The relationship between L_t and L_p was predicted to be nonlinear, but the degree of nonlinearity varied from vesicle to vesicle, depending on the vesicle dimensions and properties and the magnitude of the applied forces. For many of the tethers the data were well fit by linear regression. In all cases the slope of the L_t, L_p data pairs at the midpoint of the curve ($L_t = L_{tav}$) could be determined reliably by linear regression. The accuracy of the theoretical predictions is illustrated in Fig. 2. There were two free parameters used to fit the theoretical curve to the data: the slope of the L_t, L_p data pairs at the midpoint determined by linear regression (*dashed lines* in Fig. 2), and a vertical displacement of the curves. The different curvatures in the L_t, L_p data for different vesicles are accurately predicted by the theory (2).

Histograms showing the distributions for the calculated values of k_c, γ, k_r, and γL_t^* are shown in Fig. 3, *a–d*. In these figures each individual pull was counted as a separate observation. The values for the experimental parameters for each tethered vesicle are listed in Table 1. These values represent averages of from two to five pulls on each vesicle. The mean values for the local and nonlocal bending moduli k_c and k_r were $1.2 \pm 0.2 \times 10^{-19}$ J and $4.1 \pm 2.4 \times 10^{-19}$ J, respectively. Note that the mean value for L_t^* was essentially zero. Also note (Eqs. 7 and 8) that the value of L_t^* directly reflects errors in the absolute magnitude of the measured pressure. In view of the uncertainties in that measurement, it is likely that the distribution of values for L_t^* primarily reflects errors in the pressure measurements. These errors will also contribute to the distribution in the values of k_c. No significant difference in the parameters was observed between vesicles containing 2.0 or 10.0% POPS (student's *t* test).

Proper calculations including the nonlocal bending contribution have a significant effect on the apparent relationship between tether radius and axial force. This effect is illustrated in Fig. 4, which shows the tether

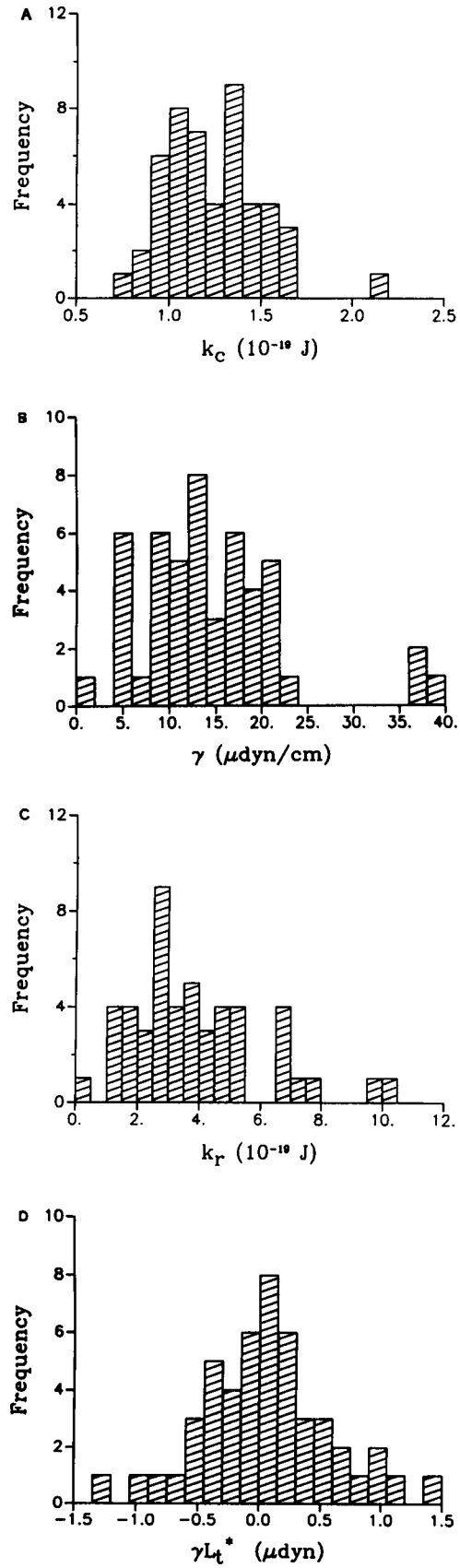

radius as a function of the force on the tether calculated with (*solid line, filled circles*) and without (*dashed line, open circles*) the nonlocal bending contribution. The curves were generated by least squares regression between the data and Eq. 5 with one free parameter, k_c. For both curves, L_t^* was taken to be zero, and for the dashed curve, γ was also taken to be zero. The value for k_c obtained by regression for the dashed curve was 1.7×10^{-19} J, consistent with the value obtained previously by this method (19). The value obtained by regression for the solid curve (i.e., including the nonlocal bending contribution) was 1.2×10^{-19} J.

DISCUSSION

These data document the importance of nonlocal stiffness in interpreting observations of tether formation from lecithin vesicles and have made it possible to make the first experimental estimates of the nonlocal bending modulus k_r, an intrinsic property of bilayer membranes. The magnitude of the nonlocal stiffness contribution is expected to increase linearly with the tether length. Thus, the experimentally relevant parameter is the nonlocal bending coefficient γ. This parameter has an important influence on the calculation of the tether radius and the intrinsic (local) bending stiffness k_c.

The coefficient k_r is expected to be related to the membrane area expansivity modulus K and the separation between neutral surfaces of the monolayers h via Eq. 4. Based on the mean value of k_r given in Table 1, and a value of 200 dyn/cm for the membrane expansivity modulus (8), the separation between the neutral surfaces of the constituent monolayers is calculated to be ~2.8 nm. According to x-ray diffraction measurements, the thickness of the membrane, including the polar head group region, is 5.0–5.6 nm (15, 23). Thus, consistent with our expectations, the calculated mean value of the separation distance between the neutral surfaces of the monolayers, h, is very nearly equal to half the thickness of the membrane. The intrinsic bending modulus k_c is also expected to be related to the membrane thickness and the area expansivity modulus. Assuming that the two monolayers act independently of each other and that for each monolayer the resistance to area expansion (or compression) is uniformly distributed over the cross section, this relationship takes the form (10, 24):

$$k_c = Kh_m^2/12, \quad (17)$$

FIGURE 3 Histograms showing the distribution of parameter values obtained in this study. Each individual pull (i.e., one cycle of increasing and decreasing tether length) was counted as one observation. The number of pulls per tether ranged from two to five.

TABLE 1 **Values of the experimental parameters**

Area (μm^2)	R_v (μm)	f (μdyn)	Δp (dyn/cm^2)	R_t (nm)	k_c (10^{-19} J)	γ (μdyn/cm)	k_t (10^{-19} J)	γL_t^* (μdyn)
10% POPS								
1230	9.0	4.10	680	20	1.0	15	4.6	−0.37
680	6.4	3.28	300	29	1.2	19	3.2	−0.22
1020	7.7	2.63	340	31	1.6	4.3	1.1	0.81
650	6.4	4.12	380	25	1.4	11	1.8	−0.46
1300	7.8	2.51	230	36	1.5	22	6.5	0.73
2070	12.0	4.20	890	20	1.2	19	10.1	0.29
1160	8.2	4.25	690	14	0.9	5.2	1.5	0.00
990	7.2	3.30	280	23	1.0	10	2.6	−0.09
1160	8.2	2.75	220	31	1.2	11	3.1	0.11
2% POPS								
1170	8.4	3.97	610	22	1.3	17	5.1	0.22
850	7.6	4.47	730	16	1.2	15	3.3	0.38
1230	8.6	3.28	250	29	1.2	12	3.6	−0.12
1100	7.5	3.05	180	34	1.0	10	2.9	−0.85
740	6.6	3.88	300	26	1.2	38	7.1	−0.26
910	6.7	2.07	90	44	0.8	20	4.5	−0.42

where h_m is the thickness of one monolayer (half the membrane thickness). Thus, the nonlocal bending modulus is expected to be approximately three times as large as the local bending stiffness. Consistent with this expectation, we obtain a ratio of the means k_r/k_c of ~3.3.

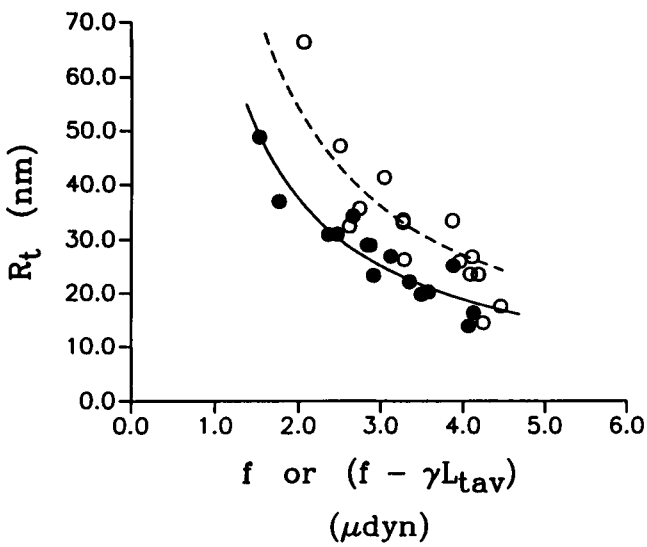

FIGURE 4 The effects of nonlocal bending stiffness on the calculation of the bending modulus, k_c. From the same data, the tether radius (at $L_t = L_{tav}$) is calculated via Eq. A5 with $\gamma = 0$ (*open symbols*) or $\gamma \neq 0$ (*filled symbols*) and plotted either as a function of force (*open symbols*) or force minus γL_{tav} (*filled symbols*). Curves were calculated by least squares regression according to Eq. 1 (*dashed curve*) or Eq. 5 (*solid curve*). For the solid curve, $\gamma L_t^* = 0$. The one free parameter in the linear regression corresponded to the membrane bending stiffness, k_c. For the dashed curve, $k_c = 1.7 \times 10^{-19}$ J; for the solid curve, $k_c = 1.2 \times 10^{-19}$ J.

The range of values for the parameter γ is quite large. Furthermore, the differences between vesicles are much greater than the variability in the values obtained from multiple measurements on the same tether, suggesting that the differences between vesicles are physical and not simply the result of measurement error. The accuracy of the theoretical prediction for the curvature of the L_p vs. L_t data supports the conclusion that these differences are physically real and significant because the predicted curvature depends primarily on the ratio γ/f_{eff} (Eq. 15), which is calculated from independent measurements of the change in the equilibrium aspiration pressure with tether length (Eqs. 9 and 11). Some differences in γ from one vesicle to the next are to be expected, because γ is an extrinsic parameter that depends on vesicle area. What is disturbing is that the expected inverse correlation between γ and area (Eq. 3) is not observed (see Fig. 5). This lack of a correlation is reflected in the range of values that we obtained for k_r. Although the mean value for k_r was consistent with our expectations, the range of values was quite broad. This is inconsistent with the notion that this parameter ought to be characteristic of membranes of a certain composition.

The physical origin of the variability remains unclear. One possibility is that the vesicles may have been multilamellar. The measurements of tether radius and the value of the local bending stiffness k_c indicate that the tether itself was formed from a single bilayer. However, it is possible that the outer, tether forming bilayer could have been associated with one or more

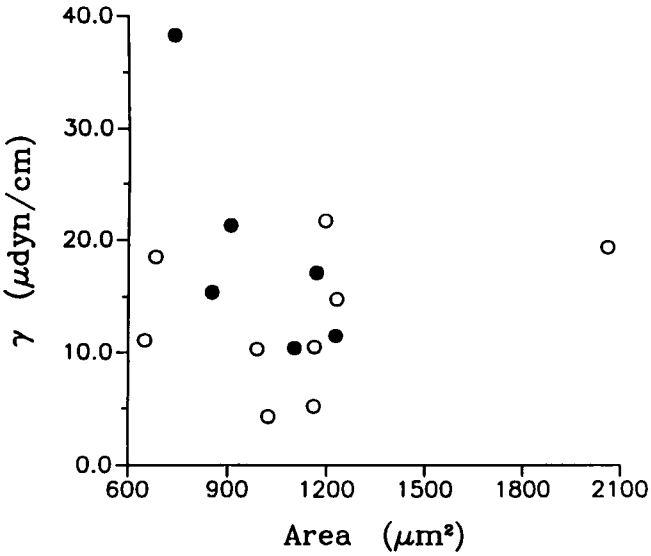

FIGURE 5 The nonlocal bending coefficient γ as a function of vesicle area. An inverse correlation according to Eq. 3 was expected, but none was observed. Solid symbols denote data from vesicles containing 2.0% POPS; open symbols, 10% POPS.

bilayers in the vesicle interior. Such additional layers might affect the value of γ because tether formation might require a reversible deformation of these inner layers. Such a deformation would result in an additional energy term in Eq. 2 corresponding to the energy required to deform the inner bilayers. This energy would depend on the stiffness of the inner layers, the number of layers involved, the closeness of their association with the tether-forming layer, and the nature of the deformations involved. Recognizing that the area of the vesicle body decreases as the tether is formed (because membrane material from the outer bilayer moves into the tether), but that the outer vesicle radius R_v actually increases as the tether forms, it is possible to imagine multilayer configurations in which inner layers might be required to expand or compress as the tether is formed. Thus, without detailed knowledge of the structure of a given vesicle, it is impossible to predict the magnitude or sign of such a contribution. Nevertheless, such a mechanism is consistent with a number of features of the data: it accounts for the fact that values for γ are consistent for a given vesicle but may be very different for different vesicles, and it explains how the distribution in the values of k_c can be narrow even though there is wide variability in the estimate of k_r.

A second possible mechanism for the variability in k_r may be that the effective area available for redistribution of molecules to or from the tether may be different from the apparent surface area of the vesicle. Such a situation might occur as a result of dynamic trapping of material in the vicinity of the tether and/or the existence of multilamellar regions on the surface that might impede lateral redistribution of the adjacent monolayers. Based on literature values for the lateral mobility of lipid molecules, we estimate that there should be sufficient time during tether formation for the redistribution to occur. For a diffusion constant of $\sim 1.0 \times 10^{-8}$ cm^2/s and a characteristic length of 10 μm, lateral redistribution should occur over a time of ~ 100 s. The time for tether formation was typically several minutes. Furthermore, for the rates of tether formation in this study, we could detect no dependence of the parameter values on formation rate. However, multilamellar structures could have affected the extent of the redistribution in some vesicles. We tried to select vesicles that appeared unilamellar, but some multilayers could have been included because of our inability to detect them microscopically.

The theoretical analysis presented in the companion report indicates that for certain dimensions of the system and membrane properties, the existence of the tether will be unstable. The conditions for instability correspond to small ratios of k_r to k_c (q) and vesicle radii that approach the radius of the pipette. Comparison of the appropriate parameters from the experiment with the predictions for instability indicate that the ratio q in the experiments is at least three times larger than the ratio q_c that marks the transition from stable to unstable configurations for the corresponding vesicle dimensions. Thus, all of these data were obtained under stable conditions.

One of the most surprising outcomes of these results is the large effect of the parameter γ on the calculated value of the intrinsic (local) bending stiffness k_c. As is evident in Fig. 4, the contribution from nonlocal bending resistance affects both the relationship between the effective "force" on the tether and the tether radius (Eq. 5) as well as the calculation of the tether radius itself (Eq. A5). The combination of these two corrections results in a 30% reduction in the calculated value of k_c. Previous calculations of k_c from measurements of tether formation did not account for these contributions (1, 19), and consequently, the reported values were larger than the actual modulus. Comparisons of those earlier measurements with the measured values of force and tether radius in this study reveal no significant differences in the data themselves, and indicate that if the data needed to calculate γ were available from those earlier studies, the results would be indistinguishable from the results of this study. The value of k_c obtained in this study agrees well with the value reported by Evans and Rawicz (9) based on micropipette measurements of thermal tensions in lecithin membranes.

This study demonstrates the importance of nonlocal bending resistance in determining the response of bi-

layer membranes to applied forces. The experimental results show that these effects are important even in vesicles with surface areas as large as 1,000 μm^2. The theoretical model predicts that the contribution from nonlocal bending rigidity will become more significant as the size of the vesicle decreases. In addition, in dynamic situations, the relative redistribution of molecules in the constituent monolayers may be limited by frictional interactions, thus limiting the effective area over which redistribution can occur over short time scales. Thus, the membrane response is expected to depend on both the size of the membrane capsule and the rate of surface deformation, the effective membrane rigidity becoming larger with decreasing size and increasing deformation rate. Recognizing the importance of these contributions and incorporating them into theoretical models will be essential for proper interpretation and accurate predictions of membrane behavior. For example, the formation of the endoplasmic reticulum is thought to involve the extrusion of lipid cylinders by microtubule-associated molecular motors. Although the characterization of some of the protein molecules involved in this process is progressing, little is known about the physical mechanisms or requirements for the formation of these structures. The magnitude of the forces and the energy required to form these cylinders is not known. While a detailed analysis of the formation of endoplasmic networks is beyond the scope of this work, the fundamental characterization of membrane properties presented here is an essential first step in understanding the physical, mechanochemical basis for the formation of such structures.

APPENDIX 1

Derivation of the expressions for the material coefficients in terms of measurable quantities involved some algebraic manipulations. The basis for the calculated relationships are the two equilibrium equations (Eqs. 5 and 6). Additional geometric relationships come from the constraints of constant area and volume:

$$R_t = R_p\left(\frac{R_p}{R_v} - 1\right)\left(\frac{dL_p}{dL_t}\right) - L_t\frac{dR_t}{dL_t} \tag{A1}$$

$$\frac{dR_v}{dL_t} = -\frac{R_p^2}{4R_v^2}\left(\frac{dL_p}{dL_t}\right). \tag{A2}$$

To obtain an expression for the effective force f_{eff}, Eqs. 5 and 6 were combined to eliminate k_c.

$$f_{eff} - \gamma L_t = \frac{2\pi\Delta p R_v R_p R_t}{R_v - R_p} \tag{A3}$$

The geometric relationship given in Eq. A1 can be substituted for R_t after the derivative dR_t/dL_t is evaluated via Eq. 5. Taking the derivative with respect to L_t of Eq. 5, we obtain:

$$\frac{dR_t}{dL_t} = \frac{\gamma R_t}{f_{eff} - \gamma L_t} \tag{A4}$$

which yields the following expression for R_t:

$$R_t = R_p\left(1 - \frac{R_p}{R_v}\right)\left(-\frac{dL_p}{dL_t}\right)\left(1 - \frac{\gamma L_t}{f_{eff}}\right). \tag{A5}$$

Substituting these results into Eq. A3 we obtain the desired expression for f_{eff} in terms of measurable quantities (Eq. 8). The expression for γ is obtained by taking the derivative of Eq. A3 with respect to L_t and using the expressions given in Eqs. A2 and A4 to obtain Eq. 9. Finally, knowing f_{eff} and γ, the modulus k_c can be calculated from the relationship obtained by combining Eqs. 5 and 6 to eliminate R_t (Eq. 10).

APPENDIX 2

Justification of the assumption that membrane area remains fixed during tether formation. The methods of calculation used in this work neglect the possibility that the area of the vesicle membrane might change during tether formation. Such a change in area might affect the calculations in two ways: first, in the calculation of the vesicle dimensions and changes in the dimensions during tether formation, it is assumed that the membrane area is constant; second, in the derivation of the equations of equilibrium from the energy variation, it is assumed that the change in energy due to variations in membrane area is small compared with energy changes resulting from other variations. This latter assumption was evaluated in a companion report (2) and the energy associated with changes in membrane area was found to be less than 1% of the energy change due to bending. To assess the potential errors that might occur in calculating vesicle dimensions, we calculate here the magnitude of the change in area that occurs during tether formation. The surface area of the vesicle is functionally related to the isotropic force resultant in the membrane, T: $\Delta A/A_o = T/K$, where A_o is the stress-free area of the membrane, ΔA is the change in area relative to A_o, and K is the expansivity modulus. The change in membrane area during tether formation can be calculated from the change in the membrane force resultant, which can in turn be calculated from the measurements of the change in aspiration pressure with increasing tether length. The largest change in pressure observed in these experiments was ~ 0.5 dyn/cm^2/μm. For a tether 300 μm in length, and a pipette radius of 0.5 μm, this corresponds to a change in membrane tension of ~ 0.075 dyn/cm. The area expansivity modulus of SOPC membrane is ~ 200 dyn/cm (8), and so the corresponding change in membrane area is 0.0375%. Clearly, such a small change in area would have a negligible effect on the calculation of the vesicle dimensions. The contribution of area change to the change in energy with tether formation under experimental conditions can also be calculated. The energy change due to a change in membrane area is: $\Delta F_A = K(\Delta A/A_o)^2/2 = \sim 1.4 \times 10^{-10}$ erg. This is small compared with the work done by the gravitational force on the bead. Even for the smallest forces used in these experiments ($\sim 2.0 \times 10^{-6}$ dyn), the work to form a 300 μm tether is $\sim 6.0 \times 10^{-8}$ erg. Thus, the assumption that the area is constant will not result in appreciable errors in the calculations.

This work was supported in part by the United States Public Health Service under NIH grants HL-18208 and HL-31524, and by the USA-Yugoslav Joint Fund, grant No. JF-888.

Received for publication 4 April 1991 and in final form 25 October 1991.

REFERENCES

1. Bo, L., and R. E. Waugh. 1989. Determination of bilayer membrane bending stiffness by tether formation from giant, thin-walled vesicles. *Biophys. J.* 55:509–517.
2. Božič, B., S. Svetina, B. Žekš, and R. E. Waugh. 1992. The role of lamellar membrane structure in tether formation from bilayer vesicles. *Biophys. J.* 61:963–973.
3. Cooper, M. S., A. H. Cornell-Bell, A. Chernjavsky, J. W. Dani, and S. J. Smith. 1990. Tubulovesicular processes emerge from trans-golgi cisternae, extend along microtubules, and interlink adjacent trans-golgi elements into a reticulum. *Cell.* 61:135–145.
4. Dabora, S. L., and M. P. Sheetz. 1988. The microtubule-dependent formation of a tubulovesicular network with characteristics of the ER from cultured cell extracts. *Cell.* 54:27–35.
5. Duwe, H.-P., H. E. Engelhardt, A. Zilker, and E. Sackmann. 1987. Curvature elasticity of smectic A lipid bilayers and cell plasma membranes. *Mol. Cryst. Liq. Cryst.* 91:1–7.
6. Evans, E. A. 1974. Bending resistance and chemically induced moments in membrane bilayers. *Biophys. J.* 14:923–931.
7. Evans, E. A., and R. M. Hochmuth. 1978. Mechanochemical properties of membranes. *In* Current Topics in Membranes and Transport. A. Kleinzeller and F. Bronner, editors. Academic Press, Inc., New York. 1–64.
8. Evans, E., and D. Needham. 1987. Physical properties of surfactant bilayer membranes: thermal transitions, elasticity, rigidity, cohesion, and colloidal interactions. *J. Phys. Chem.* 91:4219–4228.
9. Evans, E., and W. Rawicz. 1990. Entropy-driven tension and bending elasticity in condensed-fluid membranes. *Phys. Rev. Lett.* 64:2094–2097.
10. Evans, E., and R. Skalak. 1979. Mechanics and thermodynamics of biomembranes. *CRC Crit. Rev. Bioeng.* 3:181–418.
11. Faucon, J. F., M. D. Mitov, P. Meleard, I. Bivas, and P. Bothorel. 1989. Bending elasticity and thermal fluctuations of lipid membranes. Theoretical and experimental requirements. *J. Phys. (France).* 50:2389–2414.
12. Helfrich, W. 1974. Blocked lipid exchange in bilayers and its possible influence on the shape of vesicles. *Z. Naturforsch.* 29:510–515.
13. Helfrich, W. 1973. Elastic properties of lipid bilayers: theory and possible experiments. *Z. Naturforsch.* C28:693.
14. Lee, C., and L. B. Chen. 1988. Dynamic behavior of endoplasmic reticulum in living cells. *Cell.* 54:37–46.
15. McIntosh, T. J., and S. A. Simon. 1986. Hydration force and bilayer deformation: a reevaluation. *Biochemistry.* 25:4048–4066.
16. Schneider, M. B., J. T. Jenkins, and W. W. Webb. 1984. Thermal fluctuations of large cylindrical phospholipid vesicles. *Biophys. J.* 45:891–899.
17. Servuss, R. M., W. Harbich, and W. Helfrich. 1976. Measurement of the curvature-elastic modulus of egg lecithin bilayers. *Biochim. Biophys. Acta.* 436:900–903.
18. Sheetz, M. P., and S. J. Singer. 1974. Biological membranes as bilayer couples. A molecular mechanism of drug-erythrocyte interactions. *Proc. Natl. Acad. Sci. USA.* 71:4457–4461.
19. Song, J., and R. E. Waugh. 1990. Bilayer membrane bending stiffness by tether formation from mixed PC-PS lipid vesicles. *J. Biomech. Engr.* 112:235–240.
20. Sudhof, T. C. 1989. Synaptic vesicles. *Curr. Opin. Cell Biol.* 1:655–659.
21. Svetina, S., M. Brumen, and B. Žekš. 1985. Lipid bilayer elasticity and the bilayer couple interpretation of red cell shape transformations and lysis. *Stud. Biophys.* 110:177–187.
22. Svetina, S., and B. Žekš. 1989. Membrane bending energy and shape determination of phospholipid vesicles and red blood cells. *Eur. Biophys. J.* 17:101–111.
23. Torbet, J., and M. H. F. Wilkins. 1976. X-ray diffraction studies of lecithin bilayers. *J. Theor. Biol.* 62:447–458.
24. Waugh, R. E., and R. M. Hochmuth. 1987. Mechanical equilibrium of thick hollow liquid membrane cylinders. *Biophys. J.* 52:391–400.
25. Wilschut, J. 1989. Intracellular membrane fusion. *Curr. Opin. Cell Biol.* 1:639–647.